Magnetic properties of the perovskite PrMnO3: Monte Carlo Study

M.Oumarou, N.Aknin, N.Mohamedou, M.L.Ould Ne

Abstract— We study the magnetic properties of PrMnO3, the spins corresponding to the magnetic elements in this compound is given by: Pr3+(S=1) and the Mn3+ . For this study we use the Monte Carlo simulation to analyse the system within Blume-Capel model. The model is governing by an Hamiltonian that include an exchange interaction between Pr-Mn , Pr-Pr, and Mn-Mn , crystal field ,and the external field, where the reduced parameters are : r1=JPr-Pr/JPr-Mn , r2=JMn-Mn/JPr-Mn, d=Δ/JMn-Pr and h=H/JMn-Pr represent the reduced Pr-Pr, Mn-Mn exchange coupling interactions, the reduced crystal field and the reduced external magnetic field, respectively, First, in the plan: (r1,r2)We have pre sented ground state phase diagram, and we found that only stable phases are: (±2,±1), and (2,0), also we have shown the influence of parameters on a fundamental phase diagrams. Moreover, we have discussed the behavior of the magnetizations and susceptibilities of such system, also we investigated the effect of crystal field and for a different values of the latest size from N=2 to 24 of the sytem.The curie Temperature is obtained and have showed us that it is increasing when the coupling interaction increases. Furthermore, the effect of external field is presented as a hysteresis cycle loops.

Finally, we have shown that the coercive magnetic field increase when the coupling interaction increases.

Keywords— Perovskite; PrMnO3; Monte Carlo simulations; Ground state, Blume-Capel model, Magnetic properties.

1 Introduction

In the recent years Perovskite oxides (ABX3) have attracted a lot of interest in materials science, because it exhibit many peculiar properties such as superconductivity [1], ferroelectricity [2] dielectric [3], pyroelectric [4], and piezoelectric behavior [5]. These materials (ABX3) could be used in magnetic storage media, senors [6,7], and applications in spintronic devices [8], and colossal magneto resistance [9], all these properties made it fascinating as well as for fundamental perspectives and for industrial research.

In fact, this class of materials has a general chemical formula ABX3 where 'A' and 'B' are two cations and 'X' can generally be an oxide. Among these, perovskite manganite, the PrMnO3, has received a great interest in past decades due to its structural [10, 11], physical [12], and ferromagnetic [13] properties. However, the results reported by B. Bouadjemi [14], shows a half-metallic ferromagnetic ground state for PrMnO3 using GGA+U approximation. Also, the calculated structure as a function of pressure in PrMnO3 has been investigated by S. K. Mishra [15], they reported a suppression of Jahn-Teller distortion and an insulator to metal transition occurs simultaneously. Indeed, to better analyze the metal; the phase insulator transition and the CMR effect, it is important to fully understand the nature of transition.The study was motivated by the lack of investigation on the critical behaviors of the Pr-based manganites**.** One approach is to study this system by numerical methods. More recently, phase transitions of perovskite structures has been carried out by several methods such as mean field theory (MFT) [16], effective field theory (EFT) [17] and Monte Carlo (MC) simulations [18]. In Monte Carlo Simulation, we can deal various complex systems in condensed-matter physics by using random numbers and using a heat bath algorithm [19,20]**.**

The aim of this paper is to investigate the magnetic properties of PrMnO3 by Monte Carlo technique, more precisely, we present in different plan the ground state phase diagram corresponding to null temperature, also we have discussed the effect of coupling external interaction and crystal field and size on the system, the hysteresis cycle loops also have been studied.

2 The Model and Structure

Monte Carlo Method is used to study the behavior of complex spin systems**,** our study consists of two interpenetrating sublattices. One sublattice has spins σ and take the values ± 1 and 0, the other sublattice has spins S that can take four values: ± 2 , 0 , and ±1 . The spins S have only the spins σ as nearest neighbors and vice versa. The interaction between the spins σ and S is assumed to be an antiferromagnetic exchange. The Hamiltonian of the model is written as:

$$\mathcal{H} = -J_{Mn-Mn}\sum_{<i,j>} S_i S_j - J_{Pr-Pr}\sum_{<i,j>} \sigma_i \sigma_j - J_{Mn-Pr}\sum_{<i,j>} \sigma_i S_j - \Delta_1 \sum_i S_i^2 - \Delta_2 \sum_i \sigma_i^2 - H\sum (S_i + \sigma_i) \quad (1)$$

With <i, j> stand for nearest-neighbors spins, J_{Mn-Pr} is the coupling interaction constant between spins of Mn (S) and Pr (σ). J_{Mn-Mn} and J_{Pr-Pr} denote the coupling interaction constant between spins S-S and σ - σ, respectively, and the magnetic spin moment are S(Mn)=2 and σ (Pr)=1. H is the external magnetic field applied over all spins of the crystal in the z direction and Δ is the crystal field acting on the spins, this field is originated from the competition between Pr--O and Mn--O interactions.

The magnetizations per site given by:

$$m_\sigma = \frac{2}{L\times L\times L}\langle \sum_i \sigma_i \rangle \qquad (2)$$

The total magnetization is calculated by:

$$m_T = \frac{m_\sigma + m_s}{2} \qquad (3)$$

The partials and total susceptibilities can be described by:

$$\chi_s = \beta(\langle m^2{}_s\rangle - \langle m_s\rangle^2) \qquad (4)$$

.

$$\chi_\sigma = \beta(\langle m^2{}_\sigma\rangle - \langle m_\sigma\rangle^2) \qquad (5)$$

$$\chi_{tot} = \beta(\langle m^2{}_{tot}\rangle - \langle m_{tot}\rangle^2) \qquad (6)$$

Where $\beta = \frac{1}{k_B T}$, , and k_B is the Boltzmann constant, we fixed $k_B = 1$ simplicity of calculations.

We also calculate the energy of the system per site:

$$E_T = \frac{1}{L\times L\times L}\langle H \rangle \qquad (7)$$

The geometry of the studied perovskite structure is displayed in Fig.1. By simulating the model given in Eq. (1). We have carried out a Monte Carlo method in which configurations are generated by sequentially visiting all the spins in the system and free boundary conditions were imposed. Moreover, the flips are accepted or rejected according to a heat bath algorithm under a Metropolis conditions. Therefore, the system gradually achieves equilibrium after first 7000 Monte Carlo step and the data are obtained with 105 Monte Carlo Step per site (MCSS) at each temperature averaging over many initial conditions to compute the physical quantities.

3. Results and discussions

3.1 Ground state phase diagrams

In this section, we study the ground state phase diagrams corresponding to null temperature (T = 0). In fact, we discuss these phase diagrams by varying different configurations.

This system described by the Hamiltonian contains many parameters and can produce many stable topologies. These different phases are obtained by minimizing the energy value, the corresponding phase diagrams are presented in Figs. 2(a)–(f).

We present in the plan (r1, r2) in the absence of external field and for a fixed value of the crystal field Δ=1. We found only the stable configurations: (±2, ±1) and (±2,0) see Fig. 2(a),and (b) , In order to examine only the effect of the coupling interactions, we present in Fig. 2(c),and (d), The different stable phases in the absence of any external interactions. It follows from this figure that the only stable phases found are (±2,± 1), (±1,± 1), (±1,0), and for positive values of the exchange coupling r1. For negative values of this parameter, the only stable phases are identified with the states (± 2, 0) and (0, 0).

In the plane:(r2,Δ) the stables configurations are obtained, namely: (±2,± 1), (±1,± 1), (±1,± 1), (0,0), The effects of the external magnetic field H are illustrated in Figs. 2(e),and (f). From this figure it is seen that the phases are stable. These phases are: (+2,+1), (-2,-1), (+1,+1), (-1,-1), (-2,+1), (+2,-1) and (0,0), this result are obtained in the plan: :(r1,h), the second phase diagram, only six stable configurations are obtained, namely: (± 2, ±1), (± 2, 0), (± 1, ± 1), and (±1, 0),), In order to show the effect of the coupling interaction on the system we present (M ,r) in Fig.3(a)-(d). We found that the results are in good agreement with what is obtained in the phase diagrams, for a fixed value of crystal field Δ=1.and external field.

3.2 Magnetic properties

In order to examine the size effect on the magnetic properties in the absence of magnetic field.

We plot in Figs. 4(a)–(d), the total magnetization, susceptibility, specific heat and energy as a function of the reduced temperature for different values of the size from N=2 to 24, the system undergo a second order transition.

This transition occurs at reduced critical temperature given at tc, the transition gets lower for N=24 it vanishes continuously at the critical temperature, this corresponds to a peak in the susceptibility curve. The peak also increases by increasing the lattice size *N*, and it has a maximum at the transition temperature and vanishes after that taking the lowest value. In Fig. (5), we have presented the thermal behavior of partial magnetizations as well as the corresponding susceptibilities. It follows that at very low temperature values, the partial magnetizations reach their maximum values, which is in good agreement with the ground state phase diagram. Moreover, the critical temperature corresponds to a peak as it is shown in the susceptibility curves. To inspect the effect of coupling interaction r1 on the system (see Figs (6-8)), we plot in terms of reduced temperature the magnetization, specific heat and susceptibility. We reveal that the ferromagnetic state and the reduced Curie temperature increases when the coupling interaction is increasing as illustrated in Fig.9.

In order to study the effect of crystal field as illustrated in Fig .10, we plot the m for different values of r1 at h = 0. It follows from this figure the magnetization is not vanishing for values larger than Δ =- 20. Otherwise, the vanishing values of the magnetization appear at a critical value dc.

This numerical value depends on the parameter r1.In order to study the effect of the external field on the system we present

in Figs. 11–13 the hysteresis loops with different value of T, Δ, and r1. It is well known that the area underneath the hysteresis loop is equivalent to the energy converted into heat. We observe that the reduced coercive magnetic field hc increases when the reduced coupling increases. This is due to a strong exchange interaction between the Pr and Mn atoms.

Our results show that such a system becomes a hard ferrimagnetic material. Fixing the reduced exchange coupling interaction r1 and r2= 1 values and turning on the reduced crystal field, we obtain an inverse behavior compared to the previous case. This shows that this effect can be used to control the previous observed effect.

Finally, we reveal the dependency of the reduced coercive magnetic field hc in terms of the reduced exchange coupling interaction r2. . In the presence of the reduced crystal field, we found a linear behavior. It is shown that critical temperature increases when the crystal field increases.

ins:

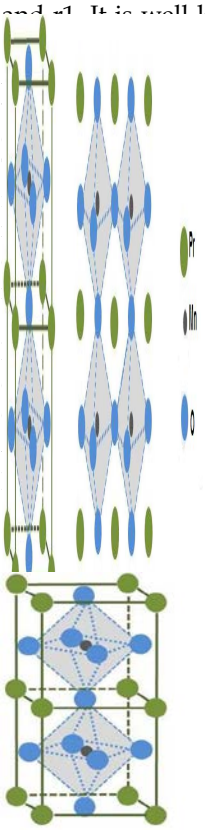

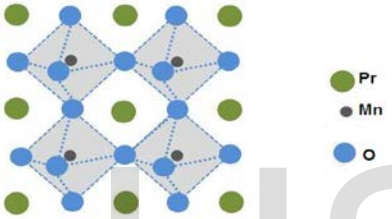

Fig .1

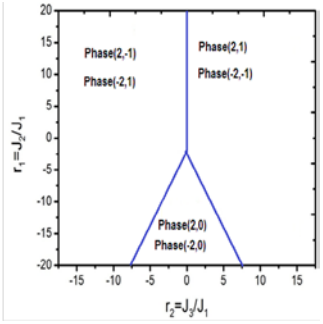

Fig.2(a)

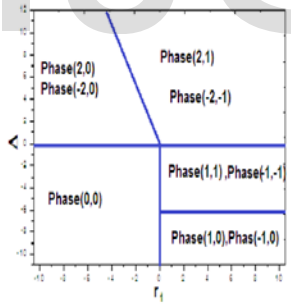

Fig.2(b)

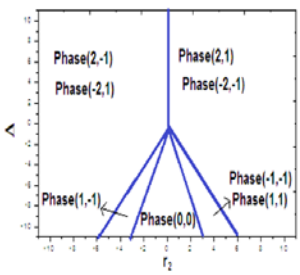

Fig.2(c)

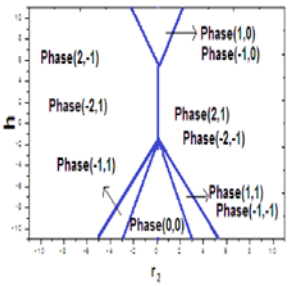

Fig.2(d)

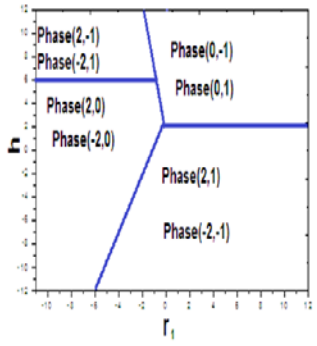

Fig.2(e)

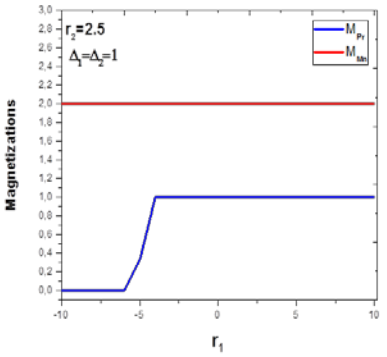

Fig.3(a)

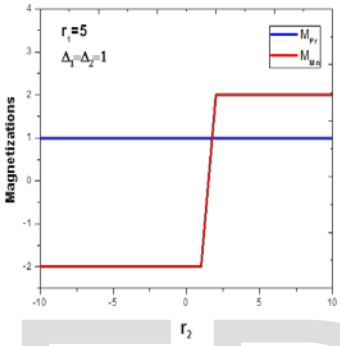

Fig.3(b)

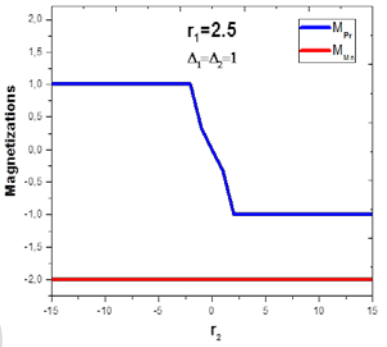

Fig.3(c)

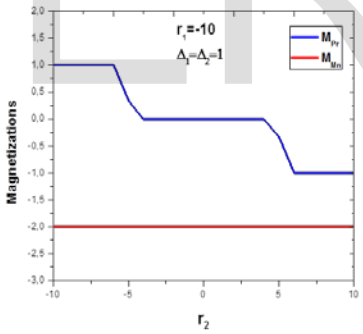

Fig.3(d)

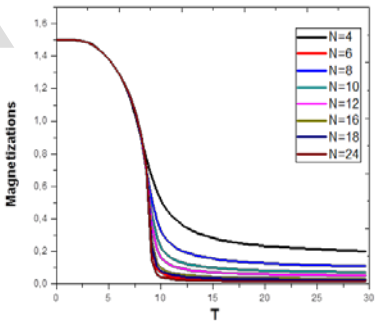

Fig.4(a)

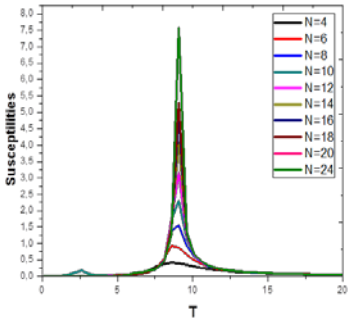

Fig.4(b)

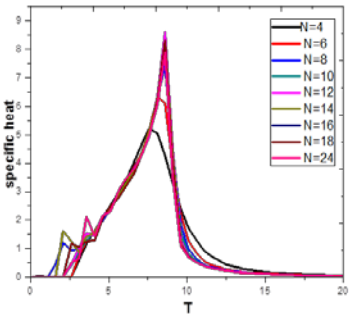

Fig.4(c)

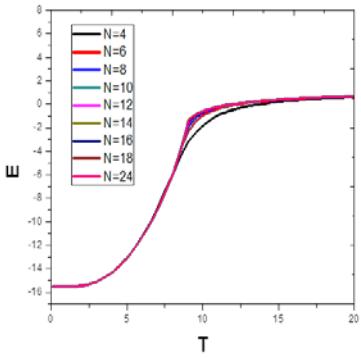

Fig.4(d)

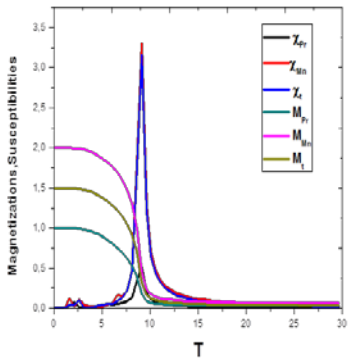

Fig.5

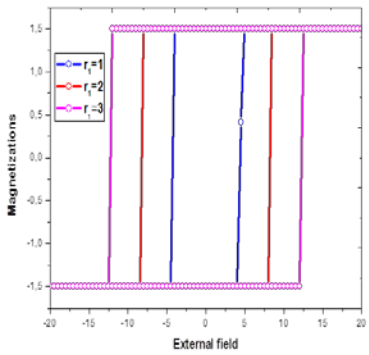

Fig.12

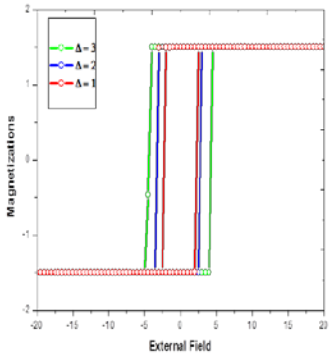

Fig.13

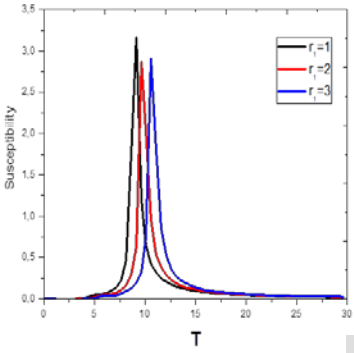

Fig.6

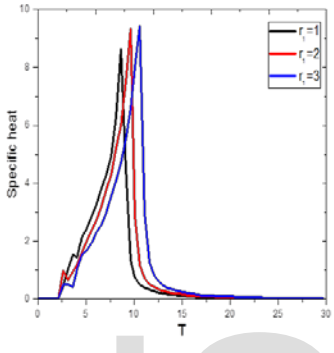

Fig.7

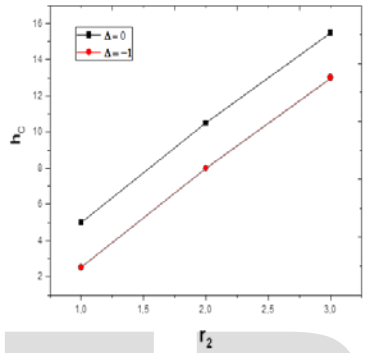

Fig.14

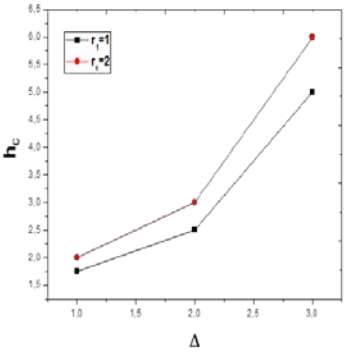

Fig.15

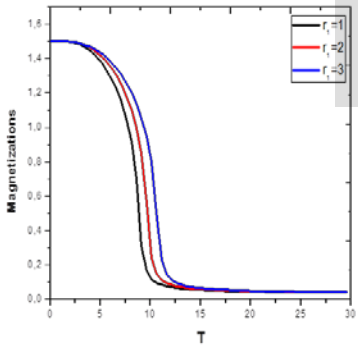

Fig.8

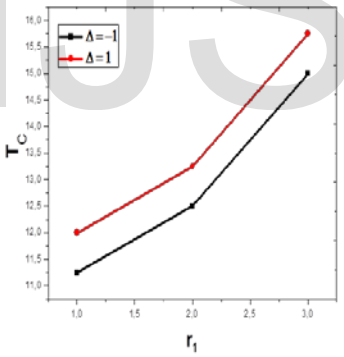

Fig.9

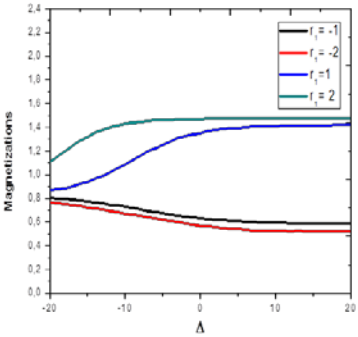

Fig.10

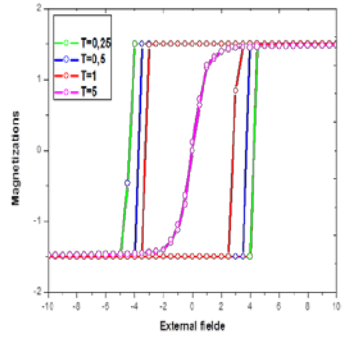

Fig.11

3.3 List of figures

Fig.1 The geometry structure of PrMnO3.

Fig.2 The ground state phase diagrams in different planes showing different configurations: (a) in the plane (r2, r1), (b) in the plane (Δ, r1). (c) In the plane (Δ, r2). (d) In the plane (h, r2), and (e) In the plane (h , Δ).

Fig.3 Magnetization as a function of the coupling- interaction for a fixed reduced of both crystal and external magnetic field Δ1=Δ2=1 and H=0: **(a)** For a fixed reduced value of coupling interaction r2 = 2.5 **(b)** For a fixed the coupling- interaction value r1 = +5.0 **(c)** For a fixed the coupling- interaction value r1 = +2.5 **(d)** For a fixed the coupling- interaction value r1 = +2.5 .

Fig.4 (**a**) The total magnetization as a function of temperature for different value of size from N= 4, to 24, for a fixed value of coupling interaction r1=r2=1.0; in the absence of the external magnetic field H=0.0 and a fixed reduced value of crystal field Δ1=Δ2=1. (b) The total Susceptibility as a function of temperature for various value of size of the system from N= 4, to 24, for a fixed reduced value of coupling interaction r1=r2=1.0; in the absence of the external magnetic field H=0.0 and crystal field Δ1=Δ2=1. (c)The total Specific heat a function of temperature for different system size values N= 4, to 24. With a fixed value of coupling interaction r1=r2=1.0; with any external magnetic field H=0.0 and crystal field Δ1=Δ2=1. (d)The total Energy, as a function of temperature for various value of system size

from N= 4, to 24. With a fixed value of coupling interaction r1=r2=1.0; in the absence of the external magnetic field H=0.0 and crystal field Δ1=Δ2=1.

Fig.5 The total and partial magnetizations and susceptibility as a function of the temperature for the cases h=0, Δ1=Δ2=1 and ar1=r2=1.

Fig.6 The total susceptibility as a function of temperature with various values of r1=1,2 and3 and a fixed value of crystal field Δ1=Δ2=1 and absence value of extern magnetic field H=0.

Fig.7 The total Specific heat as a function of temperature with various values of r1=1, 2 and3, and a fixed value of crystal field Δ1=Δ2=1 and absence value of extern field H=0.

Fig.8 The total magnetization as a function of temperature for different value of r1=1,2 and3, and a fixed value of crystal field Δ1=Δ2=1 d and absence value of extern field H=0.

Fig.9 The Curie temperature as a function of coupling interaction r1 for a fixed value of coupling interaction r2=1.0, in the absence of the external magnetic field h=0.0 and different crystal field Δ=1 and Δ=-1.

Fig.10 The total magnetization as a function of crystal field Δ1=Δ2=Δ with any external field h=0 and a fixed value of both coupling interaction r1=r2=1.

Fig.11 The total Magnetization as a function of external field with specific values of the reduced temperature T = 0.25, 0.5and 5, at a fixed reduced exchange coupling interaction r1=r2 = 1, and fixed crystal field Δ1=Δ2=1.

Fig.12 The total magnetization versus the reduced external magnetic field for different reduced exchange coupling interaction values r1=1, 2and 3; for a fixed reduced exchange coupling interaction value r2=1, in the absence of the external magnetic field h=0.0 and a fixed reduced temperature t= 0.25.

Fig.13 The total magnetization versus the external magnetic field h, for a fixed reduced temperature t=2.0: for specific values of the reduced exchange coupling interaction r1= r2=1.0, at fixed reduced temperature t= 0.25 ; in the absence of the crystal field d=0.0. for different value of crystal field Δ1=Δ2=1,2 and 3.

Fig.14 The dependency of the reduced coercive magnetic field hc in terms of the reduced exchange coupling interaction r2, for specific values of the crystal field Δ1=Δ2=0 and Δ1=Δ2=-1; for a fixed exchange coupling interaction r1=1.0,at a reduced temperature value t=0.25.

Fig .15. The dependency of the reduced coercive magnetic field hc in terms of the reduced crystal field for a fixed value of r2, for specific values of the crystal field r1=1.0 and r2=2.0; for a fixed exchange coupling interaction r2=1.0,at a reduced temperature value t=0.25.

4 Conclusion

By using Monte Carlo simulation, we have investigated the magnetic properties of the perovskite PrMnO3, in different planes : (r1, r2), (r1, Δ),(r2, Δ),(r1,h), (r2,h) and (Δ,h) we have presented ground state phase diagrams of system, and we show that the only stable configurations : (±2, ±1), (±2, 0) ,(±1, 0), ,(±1, ±1), and ,(0,0). Moreover, we discussed the thermal behavior of the magnetizations, susceptibilities, specific heat and internal energies of such system, also we found that the Curie temperature corresponding to the values of the reduced coupling interaction and the crystal field r1=r2=1, and Δ1=Δ2=1 respectively and with absence of the value of external field H=0, the hysteresis cycle loops have also been discussed.

Finally we reveal that the increasing both the Curie temperature and the coercive magnetic field and crystal field is due to the increase of the coupling interactions.

References

[1] F.S.Galasso, Structure, Properties and Preparation of Perovskite- Type Compounds, Pergamon Press, Oxford, 1969.

[2] H. Haeni, P. Irvin, W. Chang, R. Uecker, P. Reiche, Y. L. Li, S. Choudhury, W. Tian, M. E. Hawley, B. Craigo, A. K. Tagantsev, X. Q. Pan, S. K. Streiffer, L. Q. Chen, S. W. Kirchoefer, J. Levy, and D. G. Schlom, Nature, 430 [7001] 758–61 (2004).

[3] J. H. Haeni, P. Irvin, W. Chang, R. Uecker, P. Reiche, Y. L. Li, S. Choudhury, W. Tian, M. E. Hawley, B. Craigo, A. K. Tagantsev, X. Q. Pan, S. K. Streiffer , L. Q. Chen, S. W. Kirchoefer, J. Levy, and D. G. Schlom Nature 430, 758-761 (12 August 2004).

[4] J. Am. Ceram. Soc., 91; [8] 2429–2454 (2008).

[5] P. A. Salvador, A.-M. Haghiri-Gosnet, B. Mercey, M. Hervieu, and B. Raveau, "Growth and Magnetoresistive Properties of (LaMnO3)m(SrMnO3)n Superlattices," Appl. Phys. Lett., 75 [17] 2638–40 (1999).

[6] J. B. Goodenough and J. M. Longo.Crystallographic and Magnetic Properties of Perovskite and Perovskite Related Compounds. Landolt-Bornstein New Series group III, Springer Verlag, New York (1970) Vol. 4a, p. 126.

[7] M. Johnsson and P. Lemmens, in "Handbook of Magnetism and Advanced Magnetic Media",Ed. H. Kronmüller, John Wiley & Sons, New York, (2006), cond-mat/0506606.

[8] F.-X. Chem. Coudert, Mater. 2015, 27, 1905 –1916.

[9] P. Johnsson, R. Brucas, S. I. Khartsev and A.M. Grishin. Manuscript 2003.

[10] K. R. Poeppelmeier, and M. E. Leonowicz, J. C. Scanlon, J. Solid State Chem. 45, 71 (1982).

[11] A.S. Verma, A. Kumar, J. Alloys. Compd. 541 (2012) 210.

[12] D. Sousa, M. R. Nunes, C. Silveira, I. Matos, A. B. Lopes, and M. E. M. Jorge, Mater. Chem. Phys. 109, 311 (2008).

[13] X. J. Fan, H. Koinuma, and T. Hasegawa, Physica B **329–333,** 723 (2003).

[14] B. Bouadjemi, S. Bentata, A.Abbad, W.Benstaali, B.Bouhafs Solid State Communications 168 (2013) 6–10 .

[15] S. K. Mishra, M. K. Gupta, R. Mittal, A. I. Kolesnikov, S. L. Chaplot Condensed Matter > Materials Science (2005) 28.

[16] M. Arejdal, L. Bahmad, A. Abbassi, A. Benyoussef, Physica A: Statistical Mechanics and its Applications 437, 1 2015, 375–381.

[17] O. El Rhazouani , A. Benyoussef , A. El Kenz Journal of Magnetism and Magnetic Materials 377 (2015) 319-324.

[18] H. Labrim , A. Jabar , A. Belhaj , S. Ziti , L. Bahmad, L. Laânab, A. Benyous-

sef, Journal of Alloys and Compounds 641 (2015) 37–42.

[19] M. El Yadari, L. Bahmad, A. El Kenz, A. Benyoussef, Journal of Alloys and Compounds 579 (2013) 86–91.

[20] D.P. Landau, K. Binder, A Guide to Monte Carlo Simulations in Statistical Physics, Cambridge U. Press, Cambridge, 2000.